



Heriot-Watt University  
Research Gateway

## Carbon burial over the last four millennia is regulated by both climatic and land use change

### Citation for published version:

Mao, J, Burdett, HL, McGill, RAR, Newton, J, Gulliver, P & Kamenos, NA 2020, 'Carbon burial over the last four millennia is regulated by both climatic and land use change', *Global Change Biology*, vol. 26, no. 4, pp. 2496-2504. <https://doi.org/10.1111/gcb.15021>

### Digital Object Identifier (DOI):

[10.1111/gcb.15021](https://doi.org/10.1111/gcb.15021)

### Link:

[Link to publication record in Heriot-Watt Research Portal](#)

### Document Version:

Peer reviewed version

### Published In:

Global Change Biology

### Publisher Rights Statement:

This is the peer reviewed version of the following article: Mao, J, Burdett, HL, McGill, RAR, Newton, J, Gulliver, P, Kamenos, NA. Carbon burial over the last four millennia is regulated by both climatic and land use change. *Glob Change Biol.* 2020; 00: 1–9, which has been published in final form at <https://doi.org/10.1111/gcb.15021>

This article may be used for non-commercial purposes in accordance with Wiley Terms and Conditions for Use of Self-Archived Versions.

### General rights

Copyright for the publications made accessible via Heriot-Watt Research Portal is retained by the author(s) and / or other copyright owners and it is a condition of accessing these publications that users recognise and abide by the legal requirements associated with these rights.

### Take down policy

Heriot-Watt University has made every reasonable effort to ensure that the content in Heriot-Watt Research Portal complies with UK legislation. If you believe that the public display of this file breaches copyright please contact [open.access@hw.ac.uk](mailto:open.access@hw.ac.uk) providing details, and we will remove access to the work immediately and investigate your claim.

1  
2  
3  
4  
5  
6  
7  
8  
9  
10  
11  
12  
13  
14  
15  
16  
17  
18  
19  
20  
21  
22  
23  
24

# **Carbon burial over the last four millennia is regulated by both climatic and land-use change**

**Running title:** Controls on millennial-scale carbon burial

J Mao<sup>1</sup>, HL Burdett<sup>2,3</sup>, RAR McGill<sup>4</sup>, J Newton<sup>4</sup>, P Gulliver<sup>5</sup>, NA Kamenos<sup>1\*</sup>

<sup>1</sup> School of Geographical and Earth Science, University of Glasgow, Glasgow, UK

<sup>2</sup> Lyell Centre for Earth and Marine Science and Technology, Research Avenue South, Edinburgh, UK

<sup>3</sup> School of Energy, Geoscience, Infrastructure and Society, Heriot-Watt University, Edinburgh, UK

<sup>4</sup> NERC Life Sciences Mass Spectrometry Facility, Scottish Universities Environmental Research Centre, East Kilbride, Glasgow, UK

<sup>5</sup> NERC Radiocarbon Facility, Scottish Universities Environmental Research Centre, East Kilbride, Glasgow, UK

\*Corresponding author: [nick.kamenos@glasgow.ac.uk](mailto:nick.kamenos@glasgow.ac.uk)

Keywords: blue carbon, carbon burial, climate change, ecosystem shift, land use change, Little Ice Age

25 **Abstract**

26 Carbon sequestration by sediments and vegetated marine systems contributes to atmospheric  
27 carbon drawdown, but little empirical evidence is available to help separate the effects of  
28 climate change and other anthropogenic activities on carbon burial over centennial time scales.  
29 We used marine sediment organic carbon to determine the role of historic climate variability  
30 and human habitation in carbon burial over the past 5071 years. There was centennial-scale  
31 sensitivity of carbon supply and burial to climatic variability, with Little Ice Age cooling  
32 causing an abrupt ecosystem shift and an increase in marine carbon contributions compared to  
33 terrestrial carbon. Although land use changes during the late 1800s did not cause marked  
34 alteration in average carbon burial, they did lead to marked increases in the spatial variability  
35 of carbon burial. Thus, while carbon burial by vegetated systems is expected to increase with  
36 projected climate warming over the coming century, ecosystem restructuring caused by abrupt  
37 climate change may produce unexpected change in carbon burial whose variability is also  
38 modulated by land use change.

39  
40  
41  
42

## 43 **Introduction**

44

45 Coastal ecosystems represent <10% of Earth biomes (Costanza & Folke, 1997) but they play a  
46 disproportionately important role in the global carbon cycle (Bauer et al., 2013). Drawdown of  
47 atmospheric CO<sub>2</sub> into the coastal ocean enables CO<sub>2</sub> sequestration into organic tissues by  
48 photosynthesis and subsequent lock-down into sediments as sediment organic carbon (SOC)  
49 (Barbier et al., 2011; Nellemann et al., 2009). This so-called blue carbon sequestration by  
50 vegetated marine systems accounts for 50% of total marine C burial (Duarte, Middelburg, &  
51 Caraco, 2005), with fjordic sediments accounting for at least 11% of global C burial (Smith,  
52 Bianchi, Allison, Savage, & Galy, 2015), and is recognised as a potential long term store by  
53 the Intergovernmental Panel on Climate Change (IPCC) (Kennedy et al., 2013). While it is  
54 expected that climate warming may increase carbon sequestration by vegetated marine systems  
55 (Marbà, Krause-Jensen, Masqué, & Duarte, 2018), little empirical evidence is available to help  
56 separate the effects of climate change and other anthropogenic activities on carbon burial over  
57 centennial time scales. Such effects include the varying influences of alteration in  
58 allochthonous carbon sources, land use and climatic change (Fourqurean et al., 2012; Krause-  
59 Jensen et al., 2018). For example, while in terrestrial systems modelling the impacts of land  
60 use changes on carbon dynamics is increasing, in marine system climate models land use  
61 change is generally excluded (Ciais et al., 2014).

62

63 Our knowledge of carbon burial by coastal systems is greatest in their quantification, largely  
64 assessing marine habitats dominated by seagrass (e.g. (Duarte et al., 2005; Kennedy et al.,  
65 2010; Marbà et al., 2018)), salt marshes (e.g. (Chmura, Anisfeld, Cahoon, & Lynch, 2003;  
66 Kirwan & Mudd, 2012)) and mangroves (e.g. (Alongi, 2012; Bouillon et al., 2008)), SOC  
67 stored in deposits created by calcifying coralline macroalgae (Trevathan-Tackett et al., 2015;  
68 van der Heijden & Kamenos, 2015) and marine sediments storing allochthonous carbon  
69 (Smeaton et al., 2016; Smith et al., 2015). These studies have demonstrated the comparable  
70 carbon storage capacity of coastal systems to the more widely studied carbon storage  
71 ecosystems on land (e.g. rainforests) (Pidgeon, 2009). This is particularly pertinent given the  
72 temporal range over which many marine carbon repositories exist (centuries to millennia), and  
73 thus their long-term carbon accumulation potential. Over that period, biotic activity within the  
74 carbon repositories themselves can directly affect a system's capacity for carbon sequestration  
75 and burial (Mcleod et al., 2011). Additionally, damage to those systems has the capacity to not

76 only prevent sequestration but also to mobilise carbon that had been previously stored for  
77 millennia (Fourqurean et al., 2012).

78

79 Coralline algal ecosystems are a biodiverse habitat created by calcifying algae that support  
80 multiple trophic levels (Steller, Riosmena-Rodriguez, Foster, & Roberts, 2003) and have  
81 recently been highlighted as a potentially large blue carbon repository (Burrows, Kamenos,  
82 Huges, et al., 2014; van der Heijden & Kamenos, 2015). Coralline algal ecosystems are  
83 globally distributed (van der Heijden & Kamenos, 2015) and the accreted deposits they create  
84 are stable over millennia (e.g. since the early Cretaceous (Aguirre, Riding, & Braga, 2000),  
85 enabling burial and storage to occur over geological timescales. Organic carbon stored in these  
86 ecosystems is predominantly allochthonous, trapped by the complex three-dimensional nature  
87 of the algal thalli leading to deposit accretion (van der Heijden & Kamenos, 2015). Current  
88 estimates suggest net global primary production of  $173 \text{ g C m}^{-2} \text{ yr}^{-1}$  by the coralline algal  
89 component of the ecosystems (van der Heijden & Kamenos, 2015), although at present little  
90 empirical information is available on carbon burial and the balance between calcification and  
91 burial.

92

93 Here, we investigated (1) the roles of centennial scale climate and land use change in driving  
94 marine SOC accumulation and variability, (2) the longevity of carbon burial and (3) the roles  
95 of ecosystem change in driving carbon burial and variability. For this we used Loch Sween,  
96 Scotland, which has a well-defined land use history over several centuries (see Supplementary  
97 Material), is influence by major climatic variation and sequesters and stores allochthonous and  
98 autochthonous carbon in a coralline algal deposit. Sediment cores were dated using  
99 radiocarbon, and isotopic composition and C/N ratios of SOC and contemporary terrestrial /  
100 marine source end-members were determined to generate SOC stock, organic carbon source  
101 and C/N time series.

102

103

## 104 **Materials and Methods**

### 105 **Study system**

106 The coralline algal ecosystem is a highly biodiverse habitat that supports multiple trophic levels  
107 (Steller et al., 2003) and has been highlighted as a blue carbon repository (Burrows, Kamenos,  
108 Huges, et al., 2014; Trevathan-Tackett et al., 2015; van der Heijden & Kamenos, 2015).

109 Coralline algal beds are globally distributed (van der Heijden & Kamenos, 2015) and are stable  
110 over millennia (e.g. since the early Cretaceous (Aguirre et al., 2000)), enabling burial and  
111 storage to occur over geological timescales in the sediments they trap.

112

### 113 **Study site and core sampling**

114 Cores (n = 3, 11 cm diameter) were collected from a live coralline algal bed in Loch Sween  
115 (Figure S1), on the west coast of Scotland at a water depth of ~6 m. Core locations were spread  
116 across the coralline algal bed (core 1 = nearest the loch head [86 cm core length], core 2 =  
117 center of the bed [71 cm core length], core 3 = nearest the loch mouth [80 cm core length]).  
118 Cores were collected using a slide hammer and SCUBA, kept in an upright position and frozen  
119 immediately on return to shore (within 20 minutes of collection).

120

### 121 **Historic land use change**

122 Arichonan (~100 residents) was previously situated at the head of Caol Scotnish and was the  
123 primary source of nutrients into the loch. It is thought to have begun as a settlement which  
124 farmed livestock and grew crops in the 1600s. Major changes in habitation did not happen until  
125 1848 when the population of Arichonan became largely uninhabited over the following 5 years  
126 due to tenant evictions during the Highland Clearances (James, 2009).

127

### 128 **Age model**

129 Five new radiocarbon data points for Core 2 are presented in Table S1. Prior to radiocarbon  
130 dating, suitable coralline algal thalli or shell material was selected from Core 2. For each  
131 coralline algal thallus, a branch tip containing approximately 20 bands (= equivalent years of  
132 growth), was selected for analysis. Shell fragments were selected as found. Surficial calcareous  
133 encrustations were removed where necessary and the sample subjected to ultrasonic agitation  
134 in distilled water to remove detrital particles then oven dried (40 °C). In conjunction with  
135 radiocarbon dates from Core 1 (Kamenos, 2010), these new data points were used for age  
136 model construction, resulting in an age record for the past 5071 calibrated years (Tables S1 &  
137 S2).

138

139 Radiocarbon analysis was conducted at the NERC Radiocarbon Facility-East where the outer  
140 20% by weight of sample material was removed using dilute HCl. Samples were then rinsed in  
141 distilled water, dried, ground and converted to CO<sub>2</sub> via hydrolysis with 85% H<sub>3</sub>PO<sub>4</sub>. Sample  
142 CO<sub>2</sub> was cryogenically purified and an aliquot converted to graphite via Fe/Zn reduction (Slota,

143 Jull, Linick, & Toolin, 1987). Graphite was submitted to the SUERC AMS Laboratory, where  
144 sample  $^{14}\text{C}/^{13}\text{C}$  ratios were determined using a NEC 250 kV SSAMS accelerator mass  
145 spectrometer (Freeman, Dougans, McHargue, Wilcken, & Xu, 2008) and measured to 3%  
146 counting precision.

147

148 All results were appropriately background corrected and normalised to  $\delta^{13}\text{C}_{\text{VPDB}}\text{‰}$  of -25  
149 according to the conventions described in (Stuiver & Polach, 1977).  $\delta^{13}\text{C}$  concentrations were  
150 determined using a Thermo Finnigan Delta V Dual-Inlet and are representative of the  $\delta^{13}\text{C}$  of  
151 the original, pre-treated sample material.

152

153 Conventional years BP (pre-1950 AD), calibrated age ranges (BC/AD) and calibrated years BP  
154 are presented in Tables S1 and S2. Associated errors (one sigma) include components from the  
155 counting statistics on the sample, modern reference standard, process blank and instrumental  
156 error. Calibration to calendar years was conducted with OxCal version 13 (Bronk Ramsey,  
157 2009) using the Marine13 (Reimer et al., 2013) radiocarbon age calibration curve. Local  
158 deviations in the Marine Reservoir Effect were accounted for using a Delta-R of  $-47 \pm 52$  as  
159 suggested by (Russell, Cook, Ascough, & Scott, 2015). Core tops all had live coralline algal  
160 growth so were assigned a 0 years age (2015). Linear interpolation was used between dates and  
161 as the oldest part of the cores contained no datable material, linear extrapolation beyond the  
162 dated range was also used to estimate their age.

163

164 The  $^{14}\text{C}$  age model was further tuned using magnetic susceptibility (MS) performed on all core  
165 horizons (Figure S2). Direct measurements of MS (Bartington MS3E, 3.8mm spatial  
166 resolution, e.g. (Peti & Augustinus, 2019; van der Bilt et al., 2018)) were made on the flat  
167 surface of core horizons at the central portion of the core. The horizon surface was tightly  
168 covered by a single layer of plastic film during the measurement to prevent sensor  
169 contamination. Six contiguous measurements were taken on each horizon and considered as  
170 averages  $\pm$  SD. The sensor was calibrated after each measurement following manufacturer  
171 specifications.

172

### 173 **End-member sampling for isotopic calibration**

174 End member samples were collected at the sample site to enable fingerprinting of the SOC  
175 source. These included: soil (up to 15 cm depth,  $n = 5$  along an altitude gradient from the shore),

176 terrestrial plants common to the area (7 species, Table S3), partially degraded leaves found  
177 within the coralline algal bed (only *Quercus petraea* leaves were found), water column  
178 particulate organic matter (POM) (0.2  $\mu\text{m}$  seawater filtrate, n = 5), marine macroalgae (10  
179 species, see Table S4) and marine invertebrates (4 species, Table S3). Terrestrial samples were  
180 frozen immediately on collection. Marine macroalgae were gently cleaned following  
181 collection, rinsed with deionized water and frozen. Marine invertebrates were depurated in  
182 filtered seawater for 12 hours following collection, before being rinsed with deionized water  
183 and frozen.

184

### 185 **Sample preparation**

186 Each sediment core was cut into 2cm horizons whilst still frozen. Each horizon was then dried  
187 at 60°C for three days and sieved into three size fractions for subsequent SOC analysis (<63  
188  $\mu\text{m}$ , 63-250  $\mu\text{m}$ , 250-500  $\mu\text{m}$ ). Each fraction was ground into a fine powder using a ball mill  
189 and a small portion was acidified (5N HCl). Carbonate specimens (e.g. fragments of shell or  
190 coralline algae) were picked from the >500  $\mu\text{m}$  fraction for  $^{14}\text{C}$  dating (described above). All  
191 isotopic end member samples were oven dried at 60°C for three days and ground into a fine  
192 powder. Half of each powdered sample was then acidified to remove carbonate material (5N  
193 HCl), before rinsing with deionized water and drying for a second time.

194

### 195 **Stable isotope analysis**

196  $\delta^{13}\text{C}$  and  $\delta^{15}\text{N}$  stable isotope analyses was conducted at the NERC Life Sciences Mass  
197 Spectrometry Facility (at SUERC) to identify the primary source(s) of organic matter in each  
198 sediment horizon. This enabled discrimination between terrestrial / marine inputs and trophic  
199 levels via comparison to the end member samples (e.g. (Graham, Eaves, Farmer, Dobson, &  
200 Fallick, 2001; Macreadie, Allen, Kelaher, Ralph, & Skilbeck, 2012; Thornton & McManus,  
201 1994)). Since marine organisms are distinctly less cellulosic but more proteinaceous than  
202 terrestrials, C/N ratios have also been widely used for reflecting physical mixing of sediment  
203 material composited by distinct end member sources. A marine algal dominated source of  
204 sediment material is represented by C/N ratios of 4-10 (Meyers, 1994); C/N ratios >12  
205 represent terrestrial vascular plant end member sources (Lamb, Wilson, & Leng, 2006). All  
206 analyses were carried out using a Delta Plus XP continuous flow isotope ratio mass  
207 spectrometer (Thermo Fisher Scientific, Bremen, Germany) coupled to a Pyrocube Elemental  
208 Analyser (Elementar, Langenselbold, Germany). Three laboratory standards (Gelatin,  
209 Alanine/Gelatin and Glycine/Gelatin) were analysed for every 10 unknowns and used to



210 correct for instrument drift during each analytical run, which typically lasts 16 hours. Four  
211 aliquots of USGS50 were analysed each day (average and standard deviation for USGS 40 over  
212 6 analytical runs, spanning a period of 6 months (n=24) was  $\delta^{13}\text{C}$  -26.35 +/- 0.13‰ and  $\delta^{15}\text{N}$  -  
213 4.60 +/- 0.20‰, accepted values are -26.39 +/- 0.04‰ and -4.52 +/- 0.06‰ respectively).  
214 While  $\delta^{13}\text{C}$  analyses were possible for all sediment fraction sizes, only the <63  $\mu\text{m}$  fraction had  
215 sufficient N to accurately determine  $\delta^{15}\text{N}$ . SOC mass was quantified via weight percentage of  
216 organic carbon (OC%) and total carbon (TC%), determined by mass spectrometry.

217  
218  $\delta^{13}\text{C}$  and  $\delta^{15}\text{N}$  were determined in each 2 cm horizon of core 1, providing a 20-40 year  
219 resolution. For cores 2 and 3, analytical limitations prevented analysis of all the horizons: from  
220 860-150 calBP 20-40 year resolution was achieved, while horizons older and younger than this  
221 period were analysed at up to ~180 year resolution (Table S2).

222

### 223 **In situ seawater temperature**

224 A fortnightly 653-year reconstructed in-situ water temperature (IST) record for Loch Sween is  
225 available from Kamenos (2010), enabling a direct comparison between IST and carbon storage  
226 at the same location.

227

### 228 **Calculation of C stock**

229 Areal carbon storage ( $\text{Mg Ha}^{-1}$ ) was quantified using weight % organic carbon (OC), the mass  
230 of the horizon and the core surface area:

231

$$232 \quad \text{SOC}_{\text{stock}} = \sum_i S_i \times A$$

233 where,  $i$  refers to the three fractions of sediment,  $S_i$  is total SOC stock, and  $A$  is the core surface  
234 area. The SOC stock of each horizon was calculated as:

$$235 \quad S_n = WT_n \times W_n$$

236

237 where,  $n$  refers to the core horizon,  $WT$  is the weight percent of OC in each horizon, and  $W$  is  
238 the total mass of each horizon.

239

### 240 **Statistics and isotopic mixing model**

241 Data analysis was conducted in R (version 3.3.2: One-way ANOVA and Pearson correlation  
242 coefficient). The segmented package (Muggeo, 2008) was used for breakpoint regression

243 analysis, the Stable Isotope Analysis in R (SIAR) mixing model package (Parnell, 2013) for  
244 stable isotope mixing models and ggplot2 (Wickham, 2010) for visualizing data. Cross-wavelet  
245 coherence analysis was used to describe time series and compare marine in situ temperature  
246 with carbon metrics; analyses were conducted in R using the WaveletComp package (Roesch  
247 & Schmidbauer, 2014).

248  
249  
250

## 251 **Results**

252 Both organic carbon (OC) and total carbon (TC) showed a decreasing trend from the present  
253 day to ~400 calBP (Figure 1), accompanied by a distinct diversion of OC and TC during the  
254 period 400-250 calBP. As would be expected, a degree of SOC remineralisation was observed  
255 (indicated by a general decline in OC over time): this was apparent for the last ~400 years,  
256 prior to which the quantity of buried organic carbon stabilized to a constant, but lower,  
257 concentration.

258

259 While there is little evidence of a change in mean TC and OC directly after 1848 (~125 calBP),  
260 when the local habitation and livestock husbandry at Arichonan ended abruptly, there is a  
261 notable increase in OC standard deviation during the period ~1848-1950 calAD (~125-0  
262 calBP). Both TC and OC both show a marked narrowing of SD in ~125calBP (1848-50 calAD)  
263 and also ~420 calBP (~1625 calAD) (Figure 1). While these relatively short periods of reduced  
264 SD are do not directly link with troughs in IST (Figure 1), there is evidence of wider coherence  
265 between IST and OC as well as inorganic carbon (IC) and TC with a 65y period between 320-  
266 220 calBP and 150-0 calBP, and a 150y period from 250-150 calBP ( $P < 0.05$ ).

267

### 268 **Temporal change in the source of organic carbon**

269 The baseline end members provide a distinction between marine / terrestrial inputs, and across  
270 trophic levels (Figure 2). The  $\delta^{13}\text{C} / \delta^{15}\text{N}$  composition of the sediment fell into two discrete  
271 temporal periods (Figure 2); this temporal change was consistent across all cores. Prior to ~370  
272 calBP, the organic matter was characterised by lower  $\delta^{15}\text{N}$  (<6.0‰, Figure 2) and there was  
273 evidence of higher C/N elemental ratios (increased SD) (Figure 3) typical of terrestrial C3  
274 plants, suggesting that terrestrially-derived carbon was an important component of the total  
275 organic carbon pool in this system until ~370 calBP (macroalgal-derived organic material

276 (40%), terrestrial plants (28%), terrestrial soil (21%) and marine fauna (11%) (Figure S5)).  
277  $\delta^{15}\text{N}$  during this period remained relatively constant. In contrast, sediments deposited more  
278 recently than ~370 calBP were characterised by higher  $\delta^{15}\text{N}$  and  $\delta^{13}\text{C}$  typical of marine algae  
279 and fauna (Figure 2) and C/N elemental ratios were also indicative of marine-derived sources  
280 (Figure 3), suggesting a recent transition towards a dominance in marine-derived organic  
281 carbon (marine fauna (~42%), macroalgae (~27%), terrestrial plants (~24%) and terrestrial soil  
282 (~8%) (Figure S5)). Additionally, more recently than 370 calBP  $\delta^{15}\text{N}$  was characterised by a  
283 significant increase over time ( $F_{1,40}=30.1$ ,  $p<0.001$ ; Figure S4), suggesting a temporal increase  
284 in the proportional contribution of higher trophic levels to the carbon stored (i.e. derived from  
285 marine consumers, e.g. marine invertebrates).  $\delta^{13}\text{C}$  variation showed a general increase over  
286 time ( $F_{1,71}=105.9$ ,  $p<0.001$ ; Figures 2 & S3), but no clear temporal groupings in the dataset  
287 were observed. The major change in isotopic composition during ~370 calBP occurred directly  
288 after the marked drop in the in-situ temperature, but at least 200 years before the major change  
289 in habitation at Arichonan during 1848 (Figure 1). Partially degraded leaves found in the  
290 coralline algal bed were enriched in  $\delta^{15}\text{N}$  compared to their terrestrial counterparts although  
291 they still remained in the 'terrestrial' envelope. Water column particulate organic matter lay  
292 between the marine-derived and terrestrially-derived inputs (Figure 2).

293

#### 294 **Bulk carbon stock**

295 Organic carbon in coralline algal systems is associated primarily with the SOC buried in the  
296 open matrix carbonate deposits that are created by the calcifying organisms (van der Heijden  
297 & Kamenos, 2015). Within the upper 25 cm of sediment,  $7.23\pm 1.30$  (mean $\pm$ SD) Mg OC Ha<sup>-1</sup>  
298 were stored in the coralline algal bed (Figure 4). This is similar to temperate Australian  
299 seagrasses (Lavery, Mateo, Serrano, & Rozaimi, 2013) but is higher than estimates for high  
300 latitude kelp forest standing stock ( $1.41\pm 0.66$  Mg C Ha<sup>-1</sup>) (Burrows, Kamenos, Hughes, et al.,  
301 2014) and the average for high latitude marine sediments ( $2.51\pm 2.1$  Mg C Ha<sup>-1</sup>) (Burrows,  
302 Kamenos, Hughes, et al., 2014). Across the full depth of the cores, the total organic carbon  
303 (TOC) stock of the coralline algal bed was  $12.28\pm 1.98$  Mg OC Ha<sup>-1</sup>. Thus, ~60% of the TOC  
304 stock was stored in the top 25 cm of the deposit.

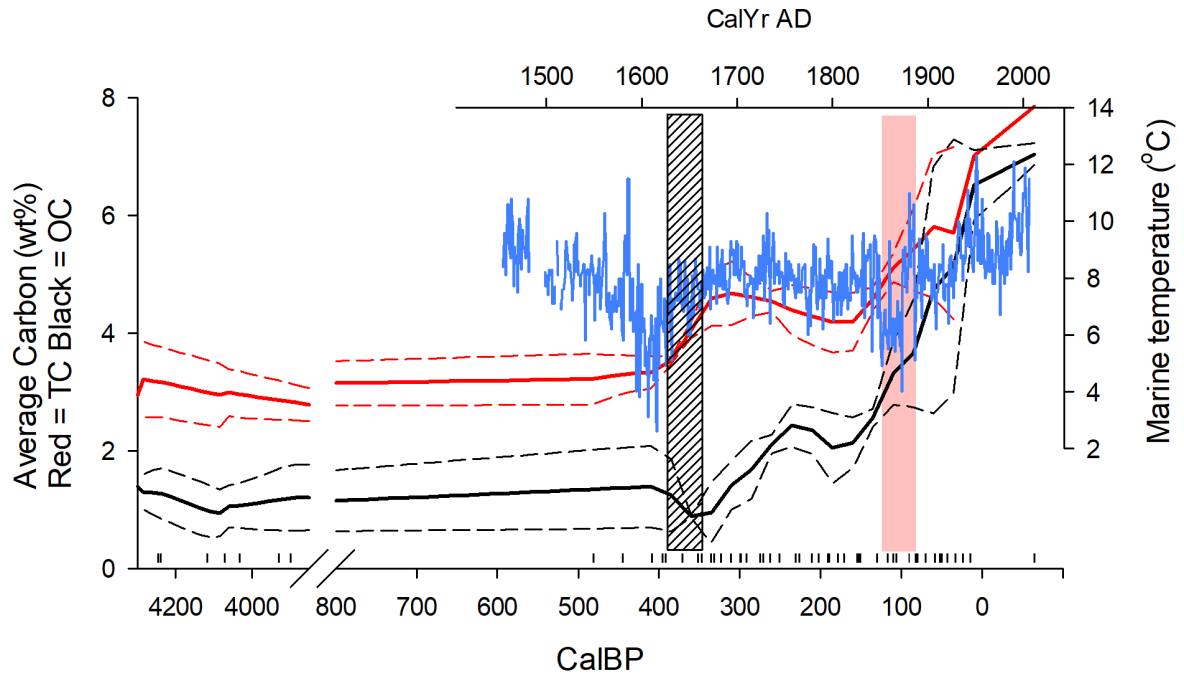
305

306

307

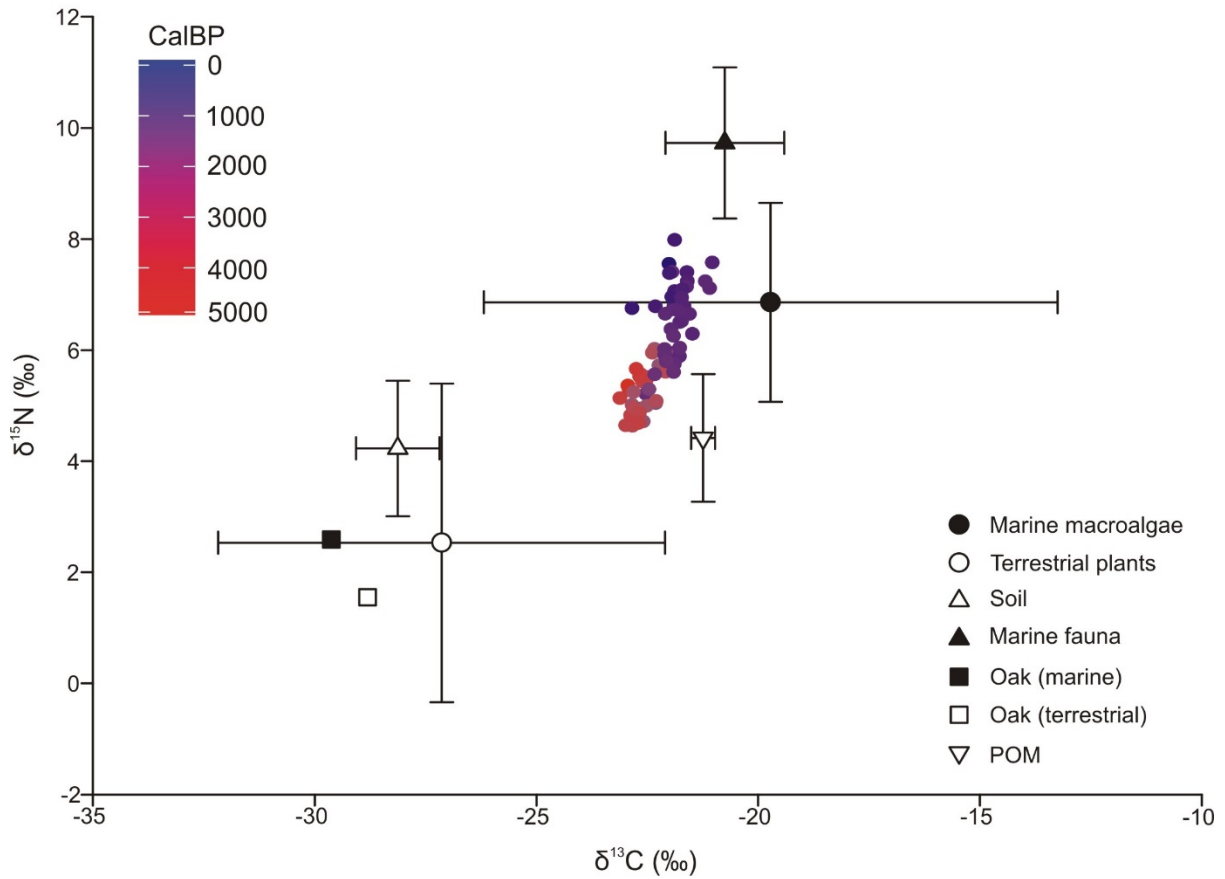
308

309  
310  
311



312  
313 **Figure 1** Average total carbon (TC, red line, n = 3 per time point), organic carbon (OC, black  
314 line, n = 3 per time point) and marine temperature (blue line). Dashed lines represent SD.  
315 Vertical rug on x axis defines calBP age of each core section used in TC and OC determination.  
316 Blue line represents in situ reconstructed marine temperature of the sampling site (Kamenos,  
317 2010). Black diagonal shading indicates period of proposed ecosystem reorganization (from  
318 Fig 2). Red shading indicates timescale of abrupt land use change.

319  
320



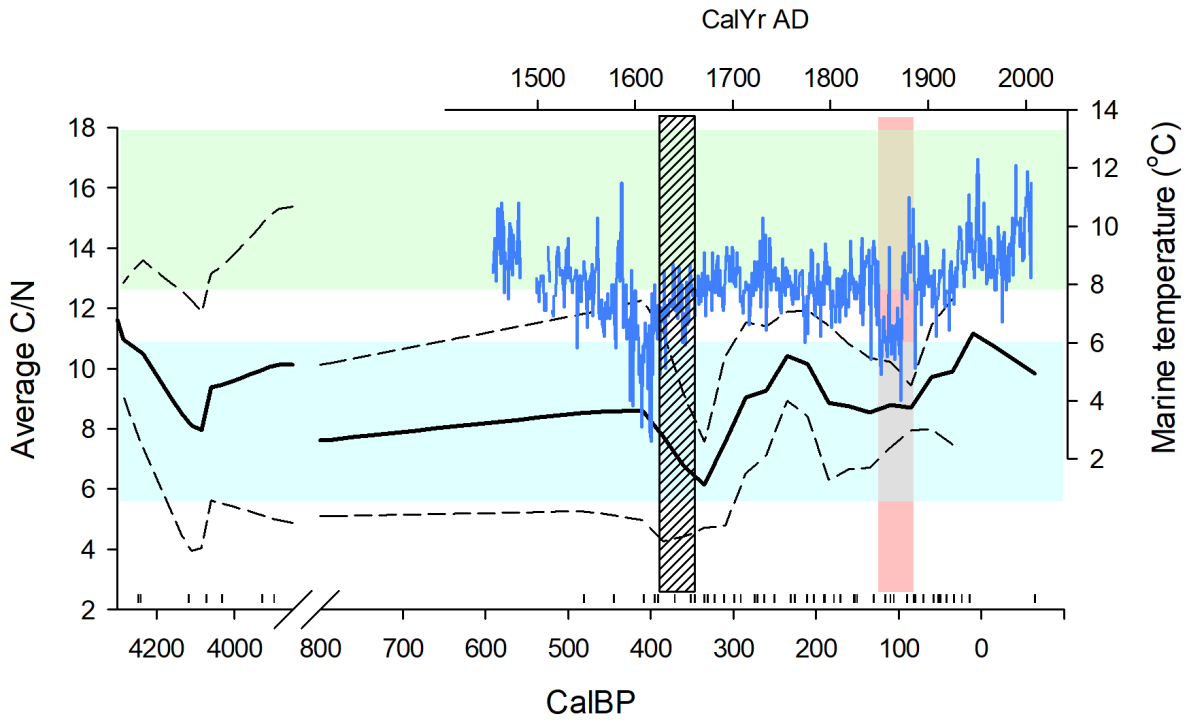
321

322

323 **Figure 2**  $\delta^{13}\text{C}$  against  $\delta^{15}\text{N}$  (‰) of core organic material (<63  $\mu\text{m}$  size fraction, coloured points,  
 324 colour-coding = sediment age) and end-members (black/white symbols, mean $\pm$ SD). ‘Oak  
 325 (marine)’ refers to fallen oak leaves that were collected underwater from within the coralline  
 326 algal bed framework. Oak was represented by 1 terrestrial and 1 marine sample so no SD  
 327 presented. POM = particulate organic matter.

328

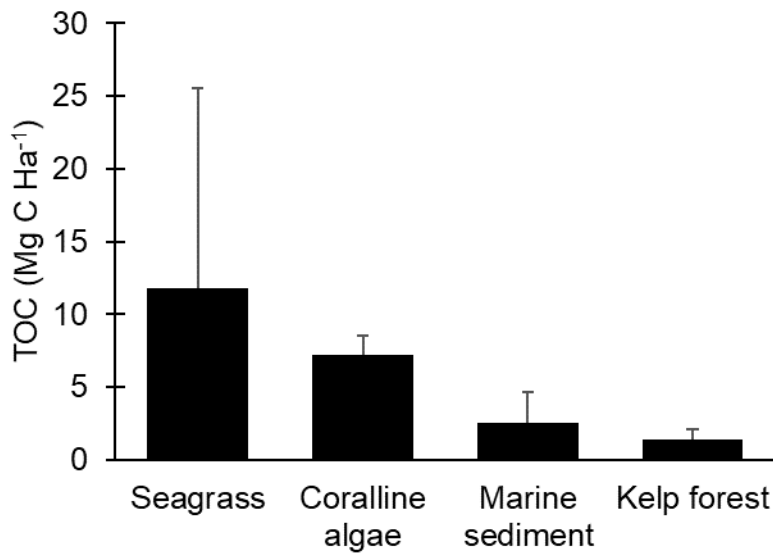
329  
330



331  
332  
333  
334  
335  
336  
337  
338  
339

**Figure 3** Soil organic material C/N elemental ratio (mean (n = 3 cores; solid line) ± SD (dashed lines)) and marine temperature (blue line; from Kamenos (2010)) over time. Vertical rug on x axis defines calBP age of each core section used to calculate C/N. Blue horizontal shading represents typical marine algal C/N ratios as defined in (Meyers, 1994). The green horizontal shading represents typical terrestrial plant C/N ratios, as defined in Lamb et al (2006). Black diagonal shading indicates period of ecosystem reorganization (from Fig 2). Red shading indicates timescale of abrupt land use change.

340



341

342 **Figure 4** Sediment organic carbon stock (TOC Mg C Ha<sup>-1</sup>) in systems classified as blue carbon  
343 repositories. Average concentrations (+SD) for top 25 cm of seagrass mats, including above-  
344 ground biomass (Lavery et al., 2013), the top 25cm of coralline algal deposits (this study) and  
345 top 25 cm of marine sediment (Burrows, Kamenos, Hughes, et al., 2014), and above-ground  
346 kelp biomass standing stock (Burrows, Kamenos, Hughes, et al., 2014).

347

348

## 349 Discussion

350

351 Here we show evidence of the influence of both historic temperature and land use changes on  
352 carbon accumulation at centennial time scales. The distinct period of low OC accumulation  
353 (starting ~370 calBP) directly followed the onset of environmental cooling during the mid-LIA  
354 temperature minimum (e.g. (Asteman, Nordberg, & Filipsson, 2013; Cage & Austin, 2010;  
355 Kamenos, 2010)), while wide variability in OC burial follows major land use changes after 125  
356 calBP.

357

### 358 Climate and land-use regulation of carbon burial

359 The coherence between OC and historic temperature variability may be driven by a decrease  
360 in organic production during periods of reduced temperature because of (1) a decrease in the  
361 metabolic rates of marine organisms (Nwewll & Northcroft, 1967) and / or (2) reduced  
362 terrestrial runoff during cooler phases, reduced nutrient delivery to marine systems and a

363 subsequent reduction in primary productivity (Szczuciński, Zajączkowski, & Scholten, 2009).  
364 This is supported by the abrupt change in the source of organic matter around ~370 calBP  
365 (Figure 2), characterised by a rapid increase in the proportional dominance of marine-derived  
366 matter and a reduction in terrestrially-derived matter. It is possible that the biological pathways  
367 linking carbon burial and climate coherence at 65y and 150y periods differ; those driving 65y  
368 period coherence being sensitive to temperature reduction while those at 150y period breaking  
369 down at higher temperatures seen during the last century (Figure 1).

370

371 Our data suggests a large, climate-driven, ecosystem shift that occurred at ~370 calBP,  
372 supported by three lines of evidence: (1) an abrupt increase in the proportion of carbon from  
373 higher trophic levels in younger sediments (Figures 2 & 3), (2) an increase in the contribution  
374 of marine-derived matter to the carbon stock in younger sediment, compared to a higher  
375 dominance of terrestrially-derived matter in older sediment (Figures S5) and (3) absence of a  
376 dramatic change in sediment composition (Figure S2), indicating that (1) and (2) happened  
377 locally and were not due to a new source of organic material derived at distance from the site.  
378 Disturbance and reorganization of ecosystems due to temperature changes are known in marine  
379 ecosystems (Gutierrez et al., 2009) and, more widely, in terrestrial ecosystems (Nolan et al.,  
380 2018); these changes can involve replacement of dominant organisms / functional types and be  
381 accelerated by other interacting processes (Hughes et al., 2007; Overpeck, Rind, & Goldberg,  
382 1990). Our data suggest that the ~370 calBP LIA-triggered ecosystem shift was associated with  
383 a relative decrease in marine productivity followed by an increase in productivity (excluding  
384 the longer-term trend driven by background remineralisation, Figure 1), further supported by  
385 the C/N ratios which become more marine after the temperature minima during the LIA (Figure  
386 3). This may be associated with a shift to a larger proportion of calcifying biota (other than the  
387 coralline algae themselves), evidenced by the divergence in TC and OC beginning around 400  
388 calBP. Notably, there is a ~50 year lag between the change in climate and the peak of ecosystem  
389 restructuring; such lags in response to climate change have also been recorded in other  
390 terrestrial and marine ecosystems and can be related to variable sensitivities of different parts  
391 of the ecosystem and associated interacting factors including population size, dependence on  
392 prey availability and resource competition (Camill & Clark, 2000; Poloczanska et al., 2016).  
393 In Caol Scotnish, this lag may be further enhanced by such interacting ecosystem processes  
394 occurring in both terrestrial and marine sources of organic material.

395

396



397

398 Just after the 125 calBP (1848-50 calAD) cooling period, OC standard deviation abruptly  
399 increased, reaching the largest SD in the record, until 0 calBP (~1950 calAD) before gradually  
400 reducing to 2015. We interpret this widening of responses as divergent influences of climate  
401 and land use changes due to human habitation on carbon burial. In 1848 the village of  
402 Arichonan (the primary source of anthropogenic inputs to Caol Scotnish) was abandoned  
403 abruptly during the Scottish Highland clearances, leaving the farmed land to rewild from its  
404 previous use in animal husbandry and arable agriculture. Our data suggest land use changes  
405 led to markedly variable organic carbon inputs, possibly due to changes in runoff patterns and  
406 the source of allochthonous carbon. This caused increased heterogeneity in carbon burial while  
407 not necessarily changing the mean quantity of carbon buried. Further, a component of that  
408 increased variability may be caused by subtly different rates of temporal organic carbon  
409 breakdown and remineralisation across the coralline algal bed during that period. Although  
410 there are two distinct periods of very reduced SD in TC and OC, these are not consistently  
411 associated with distinct climatic patterns so, given the number of replicate cores (n=3), we  
412 attribute them to chance.

413

414 In this system, land use change to farming was gradual, followed by abrupt rewilding.  
415 However, there is evidence that where habitats are damaged, losses of carbon from vegetated  
416 wetlands can be linked to eutrophication (e.g. wetlands (Hopkinson, Cai, & Hu, 2012)),  
417 dredging (seagrass (Greiner, McGlathery, Gunnell, & McKee, 2013)) as well as natural  
418 disturbances for exposed repositories including hurricanes (e.g. mangroves (Barr, Engel,  
419 Smith, & Fuentes, 2012)). Although we have little empirical evidence available for specific  
420 changes in land use during the period over which Arichonan was inhabited, the notable drop in  
421 carbon burial during 180 calBP – at which time there is no obvious thermal driver – may be  
422 due to negative changes in land use practices. Such variability in carbon release caused by  
423 changes in land use, and the way this is modelled, is a driver of differences between climate  
424 models, but this currently is not well integrated into marine modeling approaches (Ciais et al.,  
425 2014).

426

### 427 **Role of calcifying algal systems in carbon burial**

428 Relatively little is known about the role of calcified ecosystem engineers in carbon burial,  
429 where a balance exists between carbon burial and biological processes that release carbon (e.g.  
430 calcification) (van der Heijden & Kamenos, 2015). Organic carbon in these systems is

431 associated with both the calcifying engineer and associated SOC buried in the carbonate  
432 deposits that are created by the calcifying organisms. Here we have shown that the quantity of  
433 SOC buried in deposits created by calcified vegetated ecosystem engineers is comparable to,  
434 if not higher than, other vegetated systems. As would be expected, a degree of SOC breakdown  
435 and remineralisation was observed (as a general decline in OC over time). However, this was  
436 apparent for only ~500 years, after which the quantity of buried organic carbon stabilised.  
437 Importantly, coralline algal ecosystems are found throughout the world's coastal ocean, from  
438 the intertidal to 100+ m depth and their deposits are frequently stable for millennia (van der  
439 Heijden & Kamenos, 2015), representing a globally significant carbon store relevant at  
440 geological timescales. Our results show that this coastal vegetated system has persisted for at  
441 least the past 5070 years, and despite abrupt ecosystem shifts during this time, has been actively  
442 burying and storing blue carbon for the duration.

443

444 Calcifying algae can also be significant components in other vegetated systems. We now know  
445 that seagrass meadows, which are recognised blue carbon storage ecosystems (Fourqurean et  
446 al., 2012), are also globally significant 'hotspots' of calcium carbonate production because of  
447 the abundance of calcifying organisms such as epiphytes (including red coralline algae),  
448 benthic invertebrates, carbonate deposition during sedimentation, and direct carbonate  
449 formation by some seagrass species (Mazarrasa et al., 2015). Despite this potentially large  
450 source of CO<sub>2</sub> release via the calcification process, seagrass meadows likely still exhibit a net  
451 drawdown of CO<sub>2</sub> (Macreadie, Serrano, Maher, Duarte, & Beardall, 2017), demonstrating that  
452 high carbonate production does not preclude an ecosystem's role in net blue carbon storage.  
453 Thus, we suggest that calcifying algal systems may in fact represent a substantial, global-scale  
454 blue carbon repository with millennial longevity. We have shown that this carbon burial  
455 potential is sensitive to climatic variability (and subsequent biogeochemical effects) at multiple  
456 scales, including long-term climate trends, local ecological structure (e.g. terrestrial and marine  
457 primary production) and hydrogeology (e.g. sediment dynamics, river discharge).

458

## 459 **Conclusions**

460 We suggest that the quantity and variability of carbon burial is dependent upon the stability of  
461 ecosystems and their associated organic production. That relationship can be particularly  
462 complex because of the varied factors that can influence ecosystem structure, including  
463 climatic variability and, more recently, direct human impacts such as land use change and  
464 increased nutrient run-off, which can result in an increase in carbon efflux (e.g.

465 remineralization) (Macreadie et al., 2012). However, at centennial scales (the time scale over  
466 which significant amounts of carbon can accumulate) major changes in climate drives  
467 ecosystem structure and carbon burial, while land use change appears to increase the variability  
468 of carbon burial. The projected 2-4°C warming over the 21<sup>st</sup> century (IPCC, 2013) would  
469 intuitively be expected to lead to an increase in the quantity of carbon buried over coming  
470 decades, driven by concurrent increases in metabolic activity and ecosystem production.  
471 However, we suggest that such responses will likely be complicated by (1) changes in other  
472 environmental parameters (e.g. carbonate chemistry, oxygenation) projected for the end of the  
473 century (IPCC, 2013), (2) land use changes which could cause large variability in carbon burial  
474 and (3) rapid projected warming which may cause similar ecosystem reorganisation to that seen  
475 during the rapid cooling of the LIA, leading to reduced organic carbon supply despite higher  
476 productivity.

477

## 478 **Data Sharing and Data Accessibility**

479 Data used in this manuscript are available at DOI:10.17632/hgkwvww43z.1

480

## 481 **Acknowledgements**

482 Funding was obtained from the Natural Environmental Research Council UK (LSMSF/  
483 EK251-06/15 and NRCF010001 (allocation number 2001.0416)) awarded to JM, HB and NK.  
484 Henrik Stahl provided project design support and Katherine Schoenrock provided field  
485 sampling support. This publication contributes to the Scottish Blue Carbon Forum.

486

## 487 **References**

- 488 Aguirre, J., Riding, R., & Braga, J. C. (2000). Diversity of coralline red algae: origination and extinction  
489 patterns from the Early Cretaceous to the Pleistocene. *Paleobiology*, 24, 651-667.
- 490 Alongi, D. M. (2012). Carbon sequestration in mangrove forests. *Carbon Management*, 3(3), 313-322.  
491 doi:10.4155/cmt.12.20
- 492 Asteman, I., Nordberg, K., & Filipsson, H. L. (2013). The Little Ice Age: evidence from a sediment  
493 record in Gullmar Fjord, Swedish west coast. *Biogeosciences*, 10(3), 1275-1290.  
494 doi:10.5194/bg-10-1275-2013
- 495 Barbier, E. B., Hacker, S. D., Kennedy, C., Koch, E. W., Stier, A. C., & Silliman, B. R. (2011). The  
496 value of estuarine and coastal ecosystem services. *Ecological Monographs*, 81(2), 169-193.  
497 doi:10.1890/10-1510.1
- 498 Barr, J. G., Engel, V., Smith, T. J., & Fuentes, J. D. (2012). Hurricane disturbance and recovery of  
499 energy balance, CO<sub>2</sub> fluxes and canopy structure in a mangrove forest of the Florida  
500 Everglades. *Agricultural and Forest Meteorology*, 153, 54-66.  
501 doi:<https://doi.org/10.1016/j.agrformet.2011.07.022>
- 502 Bauer, J. E., Cai, W. J., Raymond, P. A., Bianchi, T. S., Hopkinson, C. S., & Regnier, P. A. (2013). The  
503 changing carbon cycle of the coastal ocean. *Nature*, 504(7478), 61-70.

504 doi:10.1038/nature12857

505 Bouillon, S., Borges, A. V., Castañeda-Moya, E., Diele, K., Dittmar, T., Duke, N. C., . . . Twilley, R. R.

506 (2008). Mangrove production and carbon sinks: A revision of global budget estimates. *Global*

507 *Biogeochemical Cycles*, 22(2), GB2013. doi:10.1029/2007gb003052

508 Bronk Ramsey, C. (2009). Bayesian Analysis of Radiocarbon Dates. *Radiocarbon*, 51(1), 337-360.

509 doi:10.1017/S0033822200033865

510 Burrows, M. T., Kamenos, N. A., Huges, D., Stahl, H., Howe, J. A., & Tett, P. (2014). *Assessment of*

511 *carbon budgets and potential blue carbon stores in Scotland's coastal and marine environment.*

512 Retrieved from Edinburgh:

513 Burrows, M. T., Kamenos, N. A., Hughes, D. J., Stahl, H., Howe, J. A., & Tett, P. (2014). Assessment

514 of carbon budgets and potential blue carbon stores in Scotland's coastal and marine

515 environment. *Scottish Natural Heritage Commissioned Report No. 761.*

516 Cage, A. G., & Austin, W. E. N. (2010). Marine climate variability during the last millennium: The Loch

517 Sunart record, Scotland, UK. *Quaternary Science Reviews*, 29(13-14), 1633-1647.

518 doi:10.1016/j.quascirev.2010.01.014

519 Camill, P., & Clark, J. S. (2000). Long-term Perspectives on Lagged Ecosystem Responses to Climate

520 Change: Permafrost in Boreal Peatlands and the Grassland/Woodland Boundary. *Ecosystems*,

521 3(6), 534-544. doi:10.1007/s100210000047

522 Chmura, G. L., Anisfeld, S. C., Cahoon, D. R., & Lynch, J. C. (2003). Global carbon sequestration in

523 tidal, saline wetland soils. *Global Biogeochemical Cycles*, 17, 1111.

524 doi:10.1029/2002GB001917

525 Ciais, P., Sabine, C. L., Bala, G., Bopp, L., Brovkin, V., Canadell, J., . . . Heimann, M. (2014). Carbon

526 and other biogeochemical cycles. In *Climate change 2013: the physical science basis.*

527 *Contribution of Working Group I to the Fifth Assessment Report of the Intergovernmental Panel*

528 *on Climate Change* (pp. 465-570): Cambridge University Press.

529 Costanza, R., & Folke, C. (1997). Valuing ecosystem services with efficiency, fairness, and

530 sustainability as goals. *Nature's services: Societal dependence on natural ecosystems*, 49-70.

531 Duarte, C. M., Middelburg, J. J., & Caraco, N. (2005). Major role of marine vegetation on the oceanic

532 carbon cycle. *Biogeosciences*, 2(1), 1-8.

533 Fourqurean, J. W., Duarte, C. M., Kennedy, H., Marba, N., Holmer, M., Mateo, M. A., . . . Serrano, O.

534 (2012). Seagrass ecosystems as a globally significant carbon stock. *Nature Geoscience*, 5(7),

535 505-509. doi:Doi 10.1038/Ngeo1477

536 Freeman, S. P. H. T., Dougans, A., McHargue, L., Wilcken, K. M., & Xu, S. (2008). Performance of the

537 new single stage accelerator mass spectrometer at the SUERC. *Nuclear Instruments and*

538 *Methods in Physics Research Section B: Beam Interactions with Materials and Atoms*, 266(10),

539 2225-2228. doi:<https://doi.org/10.1016/j.nimb.2008.02.085>

540 Graham, M. C., Eaves, M. A., Farmer, J. G., Dobson, J., & Fallick, A. E. (2001). A study of carbon and

541 nitrogen stable isotope and elemental ratios as potential indicators of source and fate of organic

542 matter in sediments of the Forth Estuary, Scotland. *Estuarine, Coastal and Shelf Science*, 52(3),

543 375-380. doi:<http://dx.doi.org/10.1006/ecss.2000.0742>

544 Greiner, J. T., McGlathery, K. J., Gunnell, J., & McKee, B. A. (2013). Seagrass Restoration Enhances

545 "Blue Carbon" Sequestration in Coastal Waters. *PloS one*, 8(8), e72469.

546 doi:10.1371/journal.pone.0072469

547 Gutierrez, D., Sifeddine, A., Field, D. B., Ortlieb, L., Vargas, G., Chavez, F. P., . . . Baumgartner, T.

548 (2009). Rapid reorganization in ocean biogeochemistry off Peru towards the end of the Little

549 Ice Age. *Biogeosciences*, 6(5), 835-848.

550 Hopkinson, C. S., Cai, W.-J., & Hu, X. (2012). Carbon sequestration in wetland dominated coastal

551 systems—a global sink of rapidly diminishing magnitude. *Current Opinion in Environmental*

552 *Sustainability*, 4(2), 186-194. doi:<https://doi.org/10.1016/j.cosust.2012.03.005>

553 Hughes, T. P., Rodrigues, M. J., Bellwood, D. R., Ceccarelli, D., Hoegh-Guldberg, O., McCook, L., . . .

554 Willis, B. (2007). Phase Shifts, Herbivory, and the Resilience of Coral Reefs to Climate Change.

555 *Current Biology*, 17(4), 360-365. doi:<https://doi.org/10.1016/j.cub.2006.12.049>

556 IPCC. (2013). *Climate Change 2013: The Physical Science Basis, Contribution of Working Group I to*

557 *the Fifth Assessment Report of the Intergovernmental Panel on Climate Change* [Stocker, T.F.,

558 D. Qin, G-K. Plattner, M. Tignor, S.K. Allen, J. Boschung, A. Nauels, Y. Xia, V. Bex and P.M.

559 Midgley (eds.]. *Cambridge University Press, Cambridge, United Kingdom and New York, NY,*  
560 *USA, 1535 pp.*

561 James, H. F. (2009). *Medieval rural settlement: a study of Mid-Argyll, Scotland.* (PhD Thesis)  
562 University of Glasgow,

563 Kamenos, N. A. (2010). North Atlantic summers have warmed more than winters since 1353, and the  
564 response of marine zooplankton. *Proceedings of the National Academy of Sciences of the*  
565 *United States of America, 107(52), 22442-22447.*  
566 doi:<http://dx.doi.org/10.1073/pnas.1006141107>

567 Kennedy, H., Alongi, D. D., Karim, A. A., Chen, G. G., Chmura, G. G., Crooks, S. S., . . . Troxler, T. T.  
568 (2013). Coastal wetlands. In *2013 Supplement to the 2006 IPCC Guidelines for National*  
569 *Greenhouse Gas Inventories: Wetlands. IPCC, Switzerland: IPCC.*

570 Kennedy, H., Beggins, J., Duarte, C. M., Fourqurean, J. W., Holmer, M., Marbà, N., & Middelburg, J.  
571 J. (2010). Seagrass sediments as a global carbon sink: Isotopic constraints. *Global*  
572 *Biogeochemical Cycles, 24(4), GB4026.* doi:10.1029/2010GB003848

573 Kirwan, M. L., & Mudd, S. M. (2012). Response of salt-marsh carbon accumulation to climate change.  
574 *Nature, 489(7417), 550-553.* doi:<https://doi.org/10.1038/nature11440>

575 Krause-Jensen, D., Lavery, P., Serrano, O., Marbà, N., Masque, P., & Duarte, C. M. (2018).  
576 Sequestration of macroalgal carbon: the elephant in the Blue Carbon room. *Biology Letters,*  
577 *14(6).* doi:10.1098/rsbl.2018.0236

578 Lamb, A. L., Wilson, G. P., & Leng, M. J. (2006). A review of coastal palaeoclimate and relative sea-  
579 level reconstructions using  $\delta^{13}\text{C}$  and C/N ratios in organic material. *Earth-Science Reviews,*  
580 *75(1), 29-57.*

581 Lavery, P. S., Mateo, M. A., Serrano, O., & Rozaimi, M. (2013). Variability in the carbon storage of  
582 seagrass habitats and its implications for global estimates of blue carbon ecosystem service.  
583 *PLoS one, 8(9), e73748.* doi:10.1371/journal.pone.0073748

584 Macreadie, P. I., Allen, K., Kelaher, B. P., Ralph, P. J., & Skilbeck, C. G. (2012). Paleoreconstruction  
585 of estuarine sediments reveal human-induced weakening of coastal carbon sinks. *Global*  
586 *Change Biology, 18(3), 891-901.* doi:10.1111/j.1365-2486.2011.02582.x

587 Macreadie, P. I., Serrano, O., Maher, D. T., Duarte, C. M., & Beardall, J. (2017). Addressing calcium  
588 carbonate cycling in blue carbon accounting. *Limnology and Oceanography Letters, 2(6), 195-*  
589 *201.*

590 Marbà, N., Krause-Jensen, D., Masqué, P., & Duarte, C. M. (2018). Expanding Greenland seagrass  
591 meadows contribute new sediment carbon sinks. *Scientific Reports, 8(1), 14024.*  
592 doi:10.1038/s41598-018-32249-w

593 Mazarrasa, I., Marbà, N., Lovelock, C. E., Serrano, O., Lavery, P. S., Fourqurean, J. W., . . . Steven, A.  
594 D. (2015). Seagrass meadows as a globally significant carbonate reservoir. *Biogeosciences.*

595 Mcleod, E., Chmura, G. L., Bouillon, S., Salm, R., Björk, M., Duarte, C. M., . . . Silliman, B. R. (2011).  
596 A blueprint for blue carbon: toward an improved understanding of the role of vegetated coastal  
597 habitats in sequestering CO<sub>2</sub>. *Frontiers in Ecology and the Environment, 9(10), 552-560.*  
598 doi:10.1890/110004

599 Meyers, P. A. (1994). Preservation of elemental and isotopic source identification of sedimentary  
600 organic matter. *Chemical Geology, 114(3-4), 289-302.* doi:10.1016/0009-2541(94)90059-0

601 Muggeo, V. M. R. (2008). Segmented: an R package to fit regression models with broken-line  
602 relationships. *R News, 8/1, 20-25.* URL <http://cran.r-project.org/doc/Rnews/>.

603 Nellemann, C., Corcoran, E., Duarte, C. M., Valdés, L., De Young, C., Fonseca, L., & Grimsditch, G.  
604 (2009). Blue Carbon - The Role of Healthy Oceans in Binding Carbon. *UN Environment,*  
605 *GRID-Arendal.*

606 Nolan, C., Overpeck, J. T., Allen, J. R. M., Anderson, P. M., Betancourt, J. L., Binney, H. A., . . . Jackson,  
607 S. T. (2018). Past and future global transformation of terrestrial ecosystems under climate  
608 change. *Science, 361(6405), 920-923.* doi:10.1126/science.aan5360

609 Nwewll, R., & Northcroft, H. (1967). A re-interpretation of the effect of temperature on the metabolism  
610 of certain marine invertebrates. *Journal of Zoology, 151(3), 277-298.*

611 Overpeck, J. T., Rind, D., & Goldberg, R. (1990). Climate-induced changes in forest disturbance and  
612 vegetation. *Nature, 343(6253), 51-53.* doi:10.1038/343051a0

613 Parnell, A., Jackson, A. (2013). siar: Stable Isotope Analysis in R. R package version 4.2.

614 Peti, L., & Augustinus, P. C. (2019). Stratigraphy and sedimentology of the Orakei maar lake sediment  
615 sequence (Auckland Volcanic Field, New Zealand). *Sci. Dril.*, 25, 47-56. doi:10.5194/sd-25-  
616 47-2019

617 Pidgeon, E. (2009). *The management of natural coastal carbon sinks*.

618 Poloczanska, E. S., Burrows, M. T., Brown, C. J., García Molinos, J., Halpern, B. S., Hoegh-Guldberg,  
619 O., . . . Sydeman, W. J. (2016). Responses of Marine Organisms to Climate Change across  
620 Oceans. *Frontiers in Marine Science*, 3(62). doi:10.3389/fmars.2016.00062

621 Reimer, P. J., Bard, E., Bayliss, A., Beck, J. W., Blackwell, P. G., Ramsey, C. B., . . . Friedrich, M.  
622 (2013). IntCal13 and Marine13 radiocarbon age calibration curves 0–50,000 years cal BP.  
623 *Radiocarbon*, 55(4), 1869-1887.

624 Roesch, A., & Schmidbauer, H. (2014). WaveletComp: Computational wavelet analysis. *R package*  
625 *version, 1*.

626 Russell, N., Cook, G. T., Ascough, P. L., & Scott, E. M. (2015). A period of calm in Scottish seas: A  
627 comprehensive study of  $\Delta R$  values for the northern British Isles coast and the consequent  
628 implications for archaeology and oceanography. *Quaternary Geochronology*, 30, 34-41.

629 Slota, P. J., Jull, A. J. T., Linick, T. W., & Toolin, L. J. (1987). Preparation of Small Samples for 14C  
630 Accelerator Targets by Catalytic Reduction of CO. *Radiocarbon*, 29(2), 303-306.  
631 doi:10.1017/S0033822200056988

632 Smeaton, C., Austin, W. E. N., Davies, A. L., Baltzer, A., Abell, R. E., & Howe, J. A. (2016). Substantial  
633 stores of sedimentary carbon held in mid-latitude fjords. *Biogeosciences*, 13(20), 5771-5787.  
634 doi:10.5194/bg-13-5771-2016

635 Smith, R. W., Bianchi, T. S., Allison, M., Savage, C., & Galy, V. (2015). High rates of organic carbon  
636 burial in fjord sediments globally. *Nature Geosci*, 8(6), 450-453. doi:10.1038/ngeo2421  
637 <http://www.nature.com/ngeo/journal/v8/n6/abs/ngeo2421.html#supplementary-information>

638 Steller, D. L., Riosmena-Rodriguez, R., Foster, M. S., & Roberts, C. A. (2003). Rhodolith bed diversity  
639 in the Gulf of California: the importance of rhodolith structure and consequences of  
640 disturbance. *Aquatic Conservation-Marine and Freshwater Ecosystems*, 13, S5-S20.  
641 doi:10.1002/aqc.564

642 Stuiver, M., & Polach, H. A. (1977). Reporting of C-14 data-Discussion. *Radiocarbon*, 19(3), 355-363.

643 Szczuciński, W., Zajączkowski, M., & Scholten, J. (2009). Sediment accumulation rates in subpolar  
644 fjords—Impact of post-Little Ice Age glaciers retreat, Billefjorden, Svalbard. *Estuarine, Coastal*  
645 *and Shelf Science*, 85(3), 345-356.

646 Thornton, S. F., & McManus, J. (1994). Application of organic carbon and nitrogen stable isotope and  
647 C/N ratios as source indicators of organic matter provenance in estuarine systems: evidence  
648 from the Tay Estuary, Scotland. *Estuarine, Coastal and Shelf Science*, 38(3), 219-233.  
649 doi:<http://dx.doi.org/10.1006/ecss.1994.1015>

650 Trevathan-Tackett, S. M., Kelleway, J., Macreadie, P. I., Beardall, J., Ralph, P., & Bellgrove, A. (2015).  
651 Comparison of marine macrophytes for their contributions to blue carbon sequestration.  
652 *Ecology*, 96(11), 3043-3057. doi:doi:10.1890/15-0149.1

653 van der Bilt, W. G. M., Rea, B., Spagnolo, M., Roerdink, D. L., Jørgensen, S. L., & Bakke, J. (2018).  
654 Novel sedimentological fingerprints link shifting depositional processes to Holocene climate  
655 transitions in East Greenland. *Global and Planetary Change*, 164, 52-64.  
656 doi:<https://doi.org/10.1016/j.gloplacha.2018.03.007>

657 van der Heijden, L., & Kamenos, N. A. (2015). Calculating the global contribution of coralline algae to  
658 total carbon burial. *Biogeosciences (BG)*, 12, 6429-6441. doi:10.5194/bg-12-6429-2015

659 Wickham, H. (2010). A layered grammar of graphics. *Journal of Computational and Graphical*  
660 *Statistics*, 19(1), 3-28.

661